JACS
JOURNAL OF THE AMERICAN CHEMICAL SOCIETY
Article
pubs.acs.org/JACS

Controlling Leakage Currents: The Role of the Binding Group and Purity of the Precursors for Self-Assembled Monolayers in the Performance of Molecular Diodes

Li Jiang,[†,‡] Li Yuan,[†,‡] Liang Cao,[†,‡] and Christian A. Nijhuis*[,†,‡]

[†]Department of Chemistry, National University of Singapore, 3 Science Drive 3, Singapore 117543
[‡]Graphene Research Centre, National University of Singapore, 2 Science Drive 3, Singapore 117542

Supporting Information

ABSTRACT: This paper describes that the performance of molecular diodes based on self-assembled monolayers (SAMs) depends on the type of anchoring group and purity of the precursors of these SAMs. The SAMs were formed on ultrasmooth template-stripped silver (Ag^{TS}) surfaces, which served as the bottom-electrode, and a eutectic alloy of gallium−indium was used as the top-electrode. When these junctions incorporate SAMs of the form $S(CH_2)_{11}Fc$ (≡ $SC_{11}Fc$) derived from $HSC_{11}Fc$, they are good molecular diodes and rectify currents with rectification ratios R (≡ $|J(-1.0\ V)|/|J(+1.0\ V)|$) of ∼$1.0 \times 10^2$. Replacing the thiol by disulfide or thioacetate functionalities in the precursor resulted in molecular diodes with values of R close to unity. Cyclic voltammetry and angle resolved X-ray photoelectron spectroscopy indicated that the SAMs derived from the disulfide or thioacetate precursors have lower surface coverages and are more defective than SAMs derived from thiols. In the junctions these defective SAMs caused defects and increased the leakage currents. The purity of the thiol-precursor is also crucial: 3 or 5% of disulfide present in the thiol caused a 28 or 61% decrease in R, respectively, and >15% of disulfide lowered R to unity, while the yield in nonshorting junctions remained unchanged. Our results show that the type of binding group, and the puritiy of the thiols, are crucial parameters in the experimental design of molecular electronic devices to ensure optimal device performance by keeping leakage currents to a minimum.

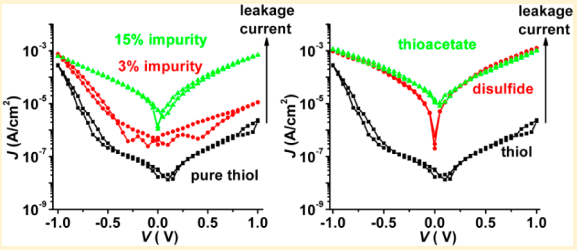

INTRODUCTION

The ability to relate the chemical and electronic structure of the organic component to the function and performance of organic and (bio)molecular electronic devices is key to designing and optimizing device performance.[1] In molecular electronics, self-assembled monolayers (SAMs),[2] or single molecules,[3,4] are the active components that can be tailored with virtually an endless number of chemical groups to provide electronic function, ranging from organic and organometallic moieties[5−11] to biological building blocks.[12−14] These building blocks form complex supramolecular structures on surfaces that depend on the outcome of a fine balance between many competing forces including molecule−substrate and inter- and intramolecular interactions. The importance of molecule−molecule interactions and packing in organic thin-film devices has been well established[15] but has not been widely investigated in SAM-based devices or junctions.[16]

Here we describe the role of the binding group of the SAM precursor in the formation of SAMs, the active component in molecular diodes (see below), on gold and silver: the anchoring group determines the supramolecular structure of the SAMs, which directly affects the leakage currents and thus the performance of molecular diodes. We used three commonly used binding groups to form SAMs on metal electrodes: thiols, disulfides, and thioacetates.[5] We fabricated molecular junctions with SAMs of the form $S\text{-}(CH_2)_{11}Fc$ (Fc = ferrocene) using $X\text{-}(CH_2)_{11}Fc$ precursors with X = SH (thiol), $SCOCH_3$ (thioacetate), and $S{-}S(CH_2)_{11}Fc$ (disulfide; see Figure 1), and we found that the performance of these molecular diodes depends strongly on the anchoring group. We believe that our results are important for the rational design of molecular electronic devices in general and show that the type of anchoring group is of crucial importance.

It is well-known from organic electronics that the device characteristics, such as the mobility of the charge carriers, depend on the packing of the polymers.[15] We have shown recently that this also applies to SAM-based junctions.[16] Consequently, the in principle "perfect" molecular architecture may result in disappointing device performance because the molecules in the SAMs cannot pack well. How the molecules pack in the monolayer, i.e., the supramolecular structure of the monolayer, depends largely, among other factors, on the binding group. Monolayers have been formed with a large number of anchoring groups tailored to immobilize the molecules on a variety of surfaces for applications in molecular electronics and in electronics more generally. For instance, thiols,[17] disulfides,[18] and thioacetates[19,20] are commonly used

Received: October 31, 2013
Published: January 8, 2014

   dx.doi.org/10.1021/ja411116n | J. Am. Chem. Soc. 2014, 136, 1982−1991

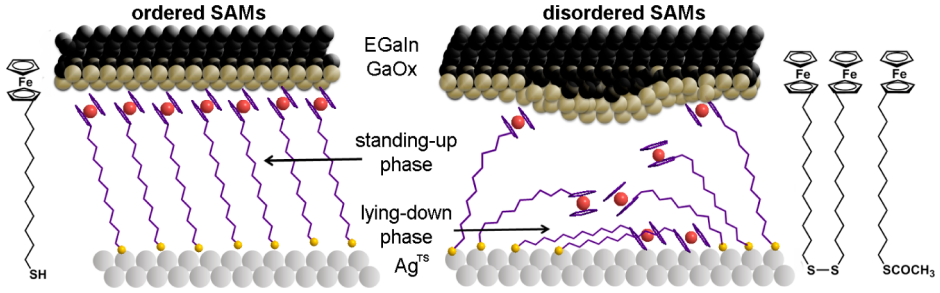

Figure 1. Schematic illustration of the junctions with SAMs derived from thiols that form well-organized SAMs and SAMs derived from disulfides or thioacetates that form disordered SAMs with domains of standing-up and lying-down phases. These junctions were formed by contacting the SAMs on Ag^{TS} bottom-electrodes by GaO_x/EGaIn top-electrodes.

to form SAMs on metals (e.g., Au, Ag, Cu, Pt, or Pd),[21] and phosphates, amines, carboxylates, or siloxanes are used for semiconductors (indium tin oxide, GaAs (001), or Si) or insulators such as glass and SiO_2.[5,22−25] Primary amines and cyano groups can also be used to form SAMs on noble metals,[26−29] and primary amines are also potentially useful to form SAMs on graphene.[30,31] Although many types of SAMs are available, the role of the anchoring group on the leakage currents has not been investigated.

Molecular rectification has been observed in junctions based on single-molecules,[9,32−35] Langmuir−Blodgett or Langmuir−Schaefer films,[36,37] and SAMs.[7,13,40,41] Metzger et al.[36−38] and others[33,39,40] have extensively studied molecular diodes of the form donor−bridge−acceptor following a model proposed by Aviram and Ratner.[41] As a group, these studies have used various anchoring groups to from monolayers, and in general the rectification ratios were low ($R < 10$) apart from a few exceptions.[36] In most studies, thioacetate or disulfide derivatives have been used because the thiol functionality is not stable and converts to the disulfide analogue in ambient conditions[42] and it may react, for instance, with an electron donor or acceptor group present within the molecule.[43] A few studies indicated that the quality of the SAMs derived from thioacetates[20,44−46] and disulfides[47,48] are of inferior quality relative to those derived from thiols. Noh et al. found that disulfides[47] and thioacetyl-protected molecules[49] formed SAMs with inhomogeneous surface morphologies and no clear domain boundaries, while thiols[50,51] formed homogeneous SAMs with sharp domain boundaries. Mihaela et al.[44] showed by STM that thioacetates form SAMs with both domains of flat-lying and standing-up molecules on Au surfaces. Chiechi et al.[52] found that SAMs derived from thioacetates are not densely packed, but the quality can be improved by using a proper base to convert the thioacetate functionality to a thiol in situ. Thus the quality of SAMs varies significantly as a function of precursor, and therefore the influence of the anchoring group on the rectification ratio, and potentially on the performance of other types of molecular junctions, is important to understand.

Figure 1 shows a schematic illustration of an "ideal" junction with a SAM of $SC_{11}Fc$ of only standing-up molecules. We formed these SAMs on ultraflat template-stripped silver (Ag^{TS}) bottom-electrodes[53] and contacted them by a nondestructive liquid-metal top-electrode of an eutectic alloy of Ga and In (75.5% Ga and 24.5% In by weight, mp = 15.7 °C, with a superficial layer of 0.7 nm of conductive GaO_x;[54] GaO_x/EGaIn).[16,55−66] The mechanism of rectification of these junctions has been reported before, and they rectify currents with rectification ratios R ($\equiv |J(-1.0\ V)|/|J(+1.0\ V)|$) of 1.0×10^2.[7,16,60,67] Therefore this molecular diode is a good model system to study the effect of the anchoring group in the performance of these diodes. These diodes block the current in one direction of bias (here at positive bias) but allow the current to pass through at opposite bias.[9,16,60,68] This feature makes it possible to study the effects of leakage currents directly (which would not be possible for junctions with simple *n*-alkanethiolates without the Fc units, which give symmetrical $J(V)$ curves) by investigating the R: the value of R decreases with increasing leakage currents at positive bias and is a sensitive indicator for leakage currents.

Figure 1 also shows a schematic illustration of a junction with a defect that lowers the distance d (nm) between the two electrodes. Here we show that this type of defect caused by the disorder of the molecules in the SAM induced by the anchoring group (flat-lying phase) results in high leakage currents, which can be rationalized as follows. Junctions can be modeled using the simplified Simmons equation (eq 1) to approximate the relationship between the tunneling current J (A/cm^2) and d where J_0 (A/cm^2) is the current density flowing through the junction for the hypothetical case of $d = 0$ and β (Å^{-1}) is the tunneling decay constant.[2,3]

$$J = J_0 e^{-\beta d} \tag{1}$$

These defects can be classified as "thin area" and "thick area" defects, according to whether the defects decrease or increase the d between the electrodes.[61,69] Eq 1 also shows that a small change in the value of d due to a defect causes an exponential change in the current density. Thick area defects lower the currents and therefore only scales with area, but thin area defects result in an exponential increase of the current and already can dominate when the junction contains small fractions of these defects.[69] Here we show that SAMs derived from disulfides and thioacetates result in diodes that do not rectify, because they contain fractions of disordered SAMs. The rectification ratios decreased by 28 or 61% for junctions with SAMs derived from thiols of $HSC_{11}Fc$ contaminated with 3 or 5% $(SC_{11}Fc)_2$, respectively, and the junctions did not rectify for disulfide fractions above 15%. These dramatic changes in the rectification ratio are caused by changes in the supramolecular structure of the SAMs induced by the anchoring group, which have a large effect on the leakage currents, but not on the yields of nonshorting junctions. Thus the yield is a poor indicator of junction quality.

EXPERIMENTAL SECTION

Ultraflat Template Surfaces. We formed ultraflat Ag and Au surfaces by a template-stripping (TS) procedure using a previously described procedure.[16,53] We deposited a layer of Ag or Au on Si/SiO_2

dx.doi.org/10.1021/ja411116n | J. Am. Chem. Soc. 2014, 136, 1982−1991

and glued glass slides on the metal surface by applying an optical adhesive (OA, Norland, No. 61), these surfaces can be stored up to a month and provide clean, ultraflat surfaces in normal laboratory conditions (see Figure S1, Supporting Information).[53,70]

Formation of SAMs. The $Fc(CH_2)_{11}SH$, $Fc(CH_2)_{11}SCOCH_3$, and $(Fc(CH_2)_{11}S)_2$ precursors for the SAMs were synthesized using procedures previously reported in the literature (see Supporting Information).[16] The Au^{TS} and Ag^{TS} substrates were immersed within 5 s after template-stripping in 3 mM ethanolic solutions of SAM precursors under an atmosphere of N_2. These ethanolic solutions were purged with N_2 gas for 15 min before the immersion of substrates. To in situ-deprotect the $FcC_{11}SCOCH_3$, we added 3 μL of 30% aqueous NH_3 (30% in H_2O by weight) per mg of thioacetate solution to the solution of $FcC_{11}SCOCH_3$ before we immersed the substrates following a procedure reported in the literature.[19] We formed the SAMs over a period of time of three hours at room temperature. Subsequently, the substrates were removed from the solutions and rinsed by ethanol and blown to dryness in a stream of N_2 gently. We used the SAM modified substrates immediately to minimize potential contamination from the ambient environment and/or deterioration of the SAMs.[7,67]

Mixed SAMs. We kept the total concentration of the precursors in ethanol at 3 mM and changed the ratio of the $Fc(CH_2)_{11}SH$ and $(Fc(CH_2)_{11}S)_2$ mixtures to obtain 0.015, 0.03, 0.05, 0.10, 0.15, 0.40, 0.60, 0.80 (fractions of molar ratios). The same procedures were followed to form SAMs on Au^{TS} and Ag^{TS} surfaces as described above.

Junction Fabrication. We followed previously reported procedure to form the junctions.[16] We used a syringe fixed on a micromanipulator (Leica, 118651, Germany) with a microneedle (Hamilton, conical shape 26s) loaded with GaO_x/EGaIn to form the cone-shaped tips of GaO_x/EGaIn. A drop of GaO_x/EGaIn was suspended from the needle and brought into contact with a sacrificial Ag^{TS} surface. By raising the needle slowly using the micromanipulator in the z-direction, the GaO_x/EGaIn drop started to deform to form two head-to-head connected cones. When these two cones separated, the syringe with the cone-shape tip of GaO_x/EGaIn suspended from it was brought into contact with the SAM-modified surface gently. The whole process was monitored by a camera (Edmund Optics, EO-3112 color USB camera), which we also used to determine the geometrical contact area of junctions (see Figure S2, Supporting Information).

Electrochemistry. We characterized the SAMs on $SC_{11}Fc$ on Au^{TS} electrodes by cyclic voltammetry (CV). The electrochemical measurements were recorded with an AUTOLAB PGSTAT302NA using NOVA 1.8 software. We used a custom built electrochemical cell with platinum counter electrode, a Ag/AgCl reference electrode, and SAM modified Au^{TS} served as a working electrode. The cyclic voltammograms were recorded at a scan rate of 1.00 V/s in aqueous 1.0 M $HClO_4$ or 1.0 M $NaClO_4$ as electrolyte solution.

Spectroscopy. Angular resolved X-ray photoemission spectroscopy (ARXPS) was performed at SINS beamline of Singapore Synchrotron Light Source equipped with a Scienta R4000 electron energy analyzer.[71] All spectra were measured at room temperature in an UHV chamber with a base pressure of 1×10^{-10} mbar. The photon energy was calibrated using the Au $4f_{7/2}$ core level peak at 84.0 eV of a sputter-cleaned gold foil in electrical contact with the sample. The binding energy is referred to the Fermi level of a sputter-cleaned gold foil.

RESULTS AND DISCUSSION

Characterization of the SAMs. In our study, we formed junctions with SAMs on Ag^{TS}, rather than on Au^{TS} because (i) Ag^{TS} surfaces have larger grain sizes than the Au^{TS} (see Figure S1, Supporting Information) and minimize defects that originate from grain boundaries, and (ii) the Ag−S−C bond angle is close to 180°, while the Au−S−C bond angle is close to 109°, which makes the molecules on Ag to stand-up more than on Au and minimizes defects that originate from phase domain boundaries. We characterized the SAMs with cyclic voltammetry (CV) and angle resolved X-ray photoelectron spectroscopy (ARXPS), but for CV we used SAMs on Au^{TS} because gold is electrochemically inert over the voltage range we applied, while silver is not and therefore complicates the interpretation of the cyclic voltammograms.

Figure 2 shows the cyclic voltammograms of SAMs on Au^{TS} derived from $HS(CH_2)_{11}Fc$, $(S(CH_2)_{11}Fc)_2$, Fc-

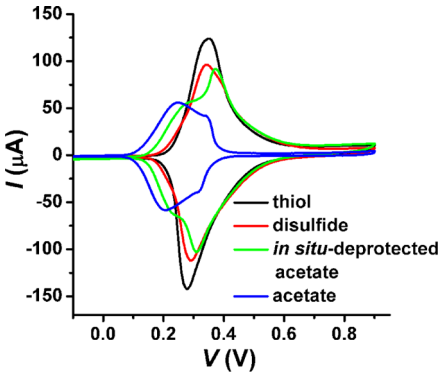

Figure 2. Cyclic voltammograms of the SAMs formed with $Fc(CH_2)_{11}SH$ (black), $(Fc(CH_2)_{11}S)_2$ (red), $Fc(CH_2)_{11}SCOCH_3$ (green) and in situ-deprotected $FcC_{11}SCOCH_3$ (blue) on Au^{TS} electrodes measured using a scan rate of 1.0 V/s, using a Ag/AgCl reference electrode and aqueous $NaClO_4$ as electrolyte.

$(CH_2)_{11}SCOCH_3$ and in situ-deprotected $FcC_{11}SCOCH_3$. We determined the surface coverage of the Fc units, Γ_{Fc} (mol/cm^2), using eq 2, where Q_{tot} is the total charge obtained by integration of the cyclic voltammogram, n is the number of electrons per mole of reaction, F is the Faraday constant (96485 C/mol), and A is the surface area of the electrode exposed to the electrolyte solution (0.33 cm^2).[72]

$$\Gamma_{Fc} = Q_{tot}/nFA \quad (2)$$

Table 1 shows that SAMs formed with $HS(CH_2)_{11}Fc$ have the highest surface coverage of Γ_{Fc} = 4.66 mol/cm^2, which is close to the theoretical value assuming hexagonal packing of the Fc moieties as spheres with a diameter of 6.6 Å (4.5×10^{-10} mol/cm^2).[73] The value of Γ_{Fc} for SAMs derived from $Fc(CH_2)_{11}SCOCH_3$ is about 31% lower than those SAMs formed by thiols; the value of Γ_{Fc} increased when the SAMs were formed by in situ-deprotection of $Fc(CH_2)_{11}SCOCH_3$ using a few drops of aqueous ammonia (30% in H_2O by weight) but is still ~10% lower than that for SAMs derived from the corresponding thiols (Table 1).

Upon oxidation of Fc moieties, the ClO_4^- anions and Fc^+ cations interact strongly and cause changes in the supramolecular structures of SAMs. For ordered SAMs with strong intermolecular van der Waals interactions, more energy is required to rearrange the SAMs, which cause an increase in the peak oxidation potentials.[16,74] Peak broadening or the appearance of shoulders or new peaks in the cyclic voltammograms indicate that the SAMs are not homogeneous.[75] Figure 2 shows that the SAMs derived from $Fc(CH_2)_{11}SCOCH_3$ have two clear redox waves that suggest that these SAMs are not homogeneous and that Fc-units are present in two distinct environments. This redox peak at lower energy is only visible as a small shoulder for SAMs derived from $(FcC_{11}S)_2$.

To investigate the supramolecular structure of these SAMs on Ag^{TS} as a function of precursor in more detail, we performed ARXPS. The S_{2p} spectra (Figure 3) are dominated by two

Table 1. Electrochemical Properties of the SAMs on Au[TS]

SAM	E_{pa} (mV)	E_{pc} (mV)	ΔE_p[a] (mV)	Γ_{Fc} ($\times 10^{-10}$ mol/cm^2)[b]
$FcC_{11}SH$	347 ± 6	279 ± 2	68 ± 6	4.66 ± 0.14
$(FcC_{11}S)_2$	344 ± 5	287 ± 3	56 ± 3	4.22 ± 0.05
$FcC_{11}SCOCH_3$	256 ± 10	215 ± 11	41 ± 2	3.21 ± 0.12
$Fc(CH_2)_{11}SCOCH_3$ + aqueous ammonia	363 ± 7	313 ± 3	50 ± 9	4.15 ± 0.24

[a] $\Delta E_p = |E_{pa} - E_{pc}|$. [b] The Γ_{Fc} was determined using eq 1.

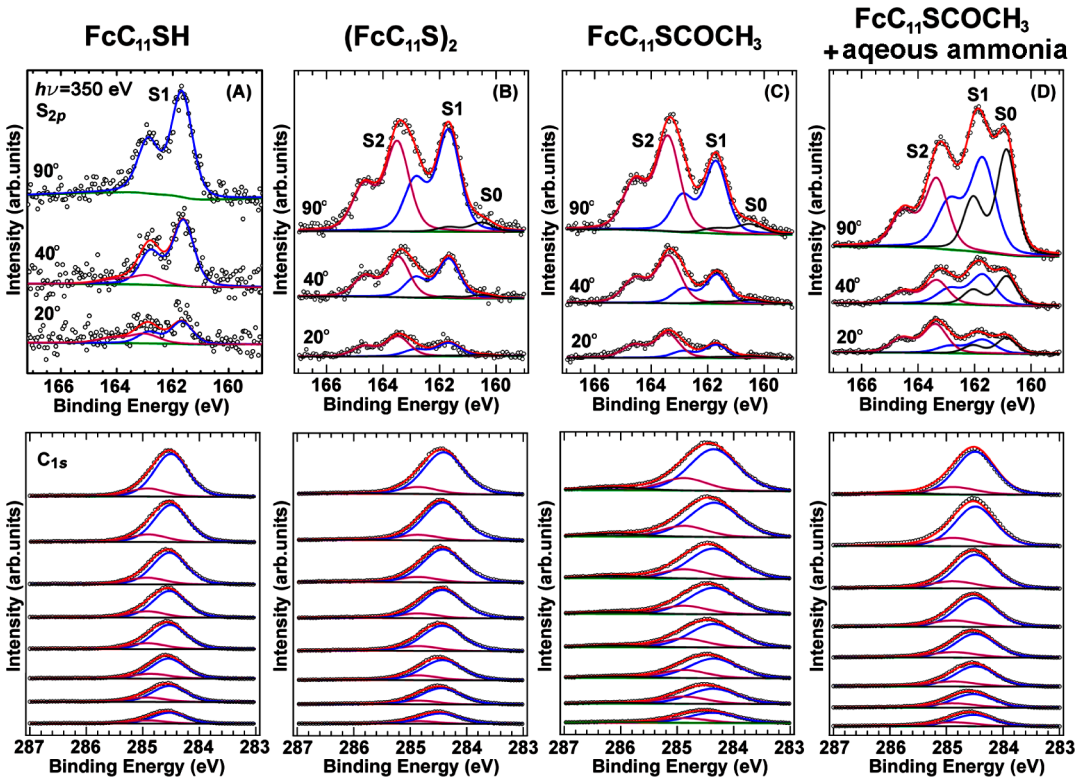

Figure 3. Angular dependent S_{2p} (from top to bottom is 90°, 40° and 20°) and C_{1s} (from top to bottom is 90°, 80°, 70°, 60°, 50°, 40°, 30° and 20°) spectra for SAMs derived from $FcC_{11}SH$ (A), $(FcC_{11}S)_2$ (B), $FcC_{11}SCOCH_3$ (C) and in situ-deprotected $FcC_{11}SCOCH_3$ (D) on Ag[TS].

components of the sulfur labeled as peak S1 and S2. For the fitting of the S_{2p} spectra, we used a splitting difference of ~1.18 eV and branching ratio of 2 ($2p_{3/2}$):1 ($2p_{1/2}$).[76] We followed previously reported peak assignments and attribute peak S1 to chemisorbed S-atoms to the surface Ag atoms and peak S2 to physisorbed molecules.[77,78] Peak S2 is more intense than S1 at grazing incidence of 20°, which indicates that the physisorbed S-atoms are not buried by SAMs. We only observed peak S1 in XPS spectra for SAMs derived from $FcC_{11}SH$, while both S1 and S2 peaks are present for SAMs derived from $FcC_{11}SCOCH_3$ and $(FcC_{11}S)_2$. For SAMs derived from $FcC_{11}SCOCH_3$ and $(FcC_{11}S)_2$, we found a small low energy peak S0. For SAMs made from in situ-deprotected $FcC_{11}SCOCH_3$, this peak dominates the spectrum. This S0 peak has been assigned to chemisorbed sulfur for disordered phases or to atomic sulfur (or other impurities) resulting from decomposition of the precursor.[77,79,80] We believe that the S0 peak reflects the presence of domains of disordered flat-lying molecules for two reasons: (i) the CV data indicate that the surface coverage of the Fc for SAMs derived from in situ-deprotected $FcC_{11}SCOCH_3$ is very similar to that for $(FcC_{11}S)_2$, and (ii) the presence of the S0 peak in the XPS data coincidences with the appearance of a new redox-wave at lower oxidation energy than the main peak in the CV data. These observations would not hold in case sulfides would have formed as a result of decomposition, because this would result in very low values of Γ_{Fc}.

We calculated the relative standing-up to laying-down phase ratio (Table 2) with respect to $FcC_{11}SH$ (assumed to be only consisting of the standing-up phase), and the average thickness of the SAMs, from the spectra of C_{1s} (see Supporting Information for details). Table 2 summarizes the average

Table 2. Relative Intensities (I_θ) at Take-Off Angles of 90° and 40° for S_{2p}, and the Thickness d and Relative Standing-Up Phase Ratio (%) from the Spectra of C_{1s} Derived from Eight Take-Off Angles in the Range of 90−20°

	S_{2p}			C_{1s}
SAM	I_θ[a] (90°) (%)	I_θ (40°) (%)	d[b] (Å)	relative standing-up phase (%)
$FcC_{11}SH$	63.4	36.6	15.3	100
$(FcC_{11}S)_2$	57.0	43.0	11.3	53
$FcC_{11}SCOCH_3$	53.1	46.9	8.9	42
$FcC_{11}SCOCH_3$+ aqueous ammonia	60.1	39.9	12.5	92

[a] I_θ is the effective intensity at different take-off angles (θ). [b] d is the average thickness of SAMs.

dx.doi.org/10.1021/ja411116n | J. Am. Chem. Soc. 2014, 136, 1982−1991

Table 3. Statistics for the Ag^{TS}-$SC_{11}Fc$//GaO_x/EGaIn Junctions

SAMs	number of junctions	number of shorts[a]	number of traces[b]	nonshorting junctions[c] (%)	rectification ratio (δ_{log}[d])
$HSC_{11}Fc$	25	2	579	92	98 (0.39)
1.5%	25	3	348	88	96 (0.24)
3%	22	3	419	86	70(0.25)
5%	20	2	431	90	38 (0.41)
10%	23	2	498	91	10 (0.24)
15%	21	2	429	90	0.64 (0.20)
40%	21	2	415	90	0.92(1.24)
60%	22	3	444	86	1.05(0.15)
80%	25	5	487	80	0.88(0.24)
$FcC_{11}SSC_{11}Fc$	23	6	534	74	0.85 (0.23)
$CH_3OCSC_{11}Fc$	26	14	616	46	1.14 (0.31)
$CH_3OCSC_{11}Fc$ + aqueous ammonia	22	3	429	87	0.58 (0.19)

[a]A short was defined when the value of J exceeded 10^2 A/cm^2 (the compliance value of J of our instrument) while recording 20 $J(V)$ scans. [b]The number of $J(V)$ traces of the Ag^{TS}-$SC_{11}Fc$//GaO_x/EGaIn Junctions. [c]The yield of nonshorting junctions is defined as the number of junctions minus the number of shorts divided by the number of junctions. [d]The δ_{log} is the log-standard deviation.

thickness and relative phase domain ratios of the SAMs derived from the ARXPS spectra and summarize two important observations: (i) SAMs derived from $FcC_{11}SCOCH_3$ or $(FcC_{11}S)_2$ generated the smallest fractions of standing-up phase and yielded SAMs with the smallest average thickness, and (ii) in situ-deprotection of the $FcC_{11}SCOCH_3$ precursor improved the quality of the SAMs but are still inferior to SAMs derived from $FcC_{11}SH$ thiols. These results correspond very well to the surface coverage determined by CV and the XPS data discussed above and confirm that SAMs derived from disulfides and thioacetates are inferior to those derived from thiols.

Performance of the Molecular Diodes as a Function of Binding Group. We fabricated junctions of the form Ag^{TS}-$X(CH_2)_{11}Fc$//GaO_x/EGaIn with X = SH, $SCOCH_3$, or X = S−$S(CH_2)_{11}Fc$ to investigate their electronic properties as function of anchoring group. In these junctions, the role of the thin (0.7 nm)[54] self-limiting GaO_x layer that forms spontaneously on the bulk alloy has been well-characterized. This GaO_x layer (i) stabilizes the bulk metal in nonspherical shapes and prevents it from alloying with the bottom-electrode,[81] (ii) contains oxygen vacancies, is highly conductive, and forms Ohmic-contacts with SAMs and other types of surfaces,[60,67,82] and (iii) adds mechanical stability because of its non-Newtonian properties.[60,67,81] Whitesides et al. recently showed the effective electrical contact area is lower than the geometrical contact area, but the contact area is highly reproducible and remains constant. These features of the "EGaIn-technique" make it a very useful tool conduct physical-organic studies of charge transport across SAM-based junctions with statistically large numbers of data.[83]

We measured and analyzed statistically large numbers of data (Table 3; one trace ≡ 0 V→ 1.0 V→ −1.0 V → 0 V) following previously reported procedures.[16] We determined the log-average values of J for each potential at which J was measured, which we used to construct the log-average $J(V)$ curves (see Supporting Information).[7] Figure 4 shows the log-average $J(V)$ curves. Junctions formed with SAMs derived from the thiols perform well and rectify currents with values of R of 98 with 92% yield in nonshorting devices. These characteristics are similar to previously reported characteristics for these junctions.[7,16,60,67] In contrast, junctions that incorporated SAMs formed with thioacetates, in situ-deprotected thioacetate, or disulfide precursors did not perform well and rectified currents with values of R close to unity. There are some outliers in the histograms, which are mainly caused by one or two unstable junctions or drifting of the top electrodes.[16,83]

Figure 5A shows both the surface coverage and the yield in nonshorting junctions as a function of the four types of SAM precursors. The yield of nonshorting junctions is high (close to 90%) when the surface coverage of Fc units is close the theoretical maximum (4.5×10^{-10} mol/cm^2) and low (46%) when the surface coverage is low (3.2×10^{-10} mol/cm^2). The high yields in nonshorting junctions, however, do not correlate with the rectification ratio. Thus, the yield of nonshorting devices is a poor indicator of the quality of the junctions.

Figure 5B shows the values of J determined at a bias at −1.0 V, when the diodes are in the on-state and allow the current to pass through the junction, and at +1.0 V, when the diodes are in the off-state and block the current. This figure shows that the current densities of all junctions at −1.0 V are (nearly) the same, while the leakage currents at +1.0 V varies over 2 orders of magnitude. Thus the junctions formed with SAMs derived from disulfide or thioacetate precursor do not rectify because they do not block the current efficiently in the off-state. In the off-state, the Fc moiety is part of the tunneling barrier, while in the on-state the Fc units are a hopping center. When the molecules in the SAMs are loosely packed, or disordered, they are more prone to defects during fabrication and block the current less efficiently at positive bias. These results show that the lower quality of the SAMs derived from disulfides and thioacetates have a dramatic effect on the leakage currents across the junctions. This effect is so large because of the exponential dependence of the currents on the effective distance between two electrodes (eq 1).

Role of Impurities. The previous sections describe the importance of the supramolecular structure of the SAMs in the performance of molecular diodes: SAMs derived from the disulfides yield molecular diodes that do not rectify currents, while SAMs derived from thiols yields junctions that perform well. Thiols convert to disulfides in ambient conditions and are the most common impurity in, for instance, commercially available thiols.[42] On the basis of the results described above, we hypothesize that contamination of the thiols with even small quantities of disulfides may impede the quality of the SAMs and the performance of the molecular diode. To investigate the potential role of disulfide impurities in the thiol precursor in the performance of the molecular diodes, we intentionally added

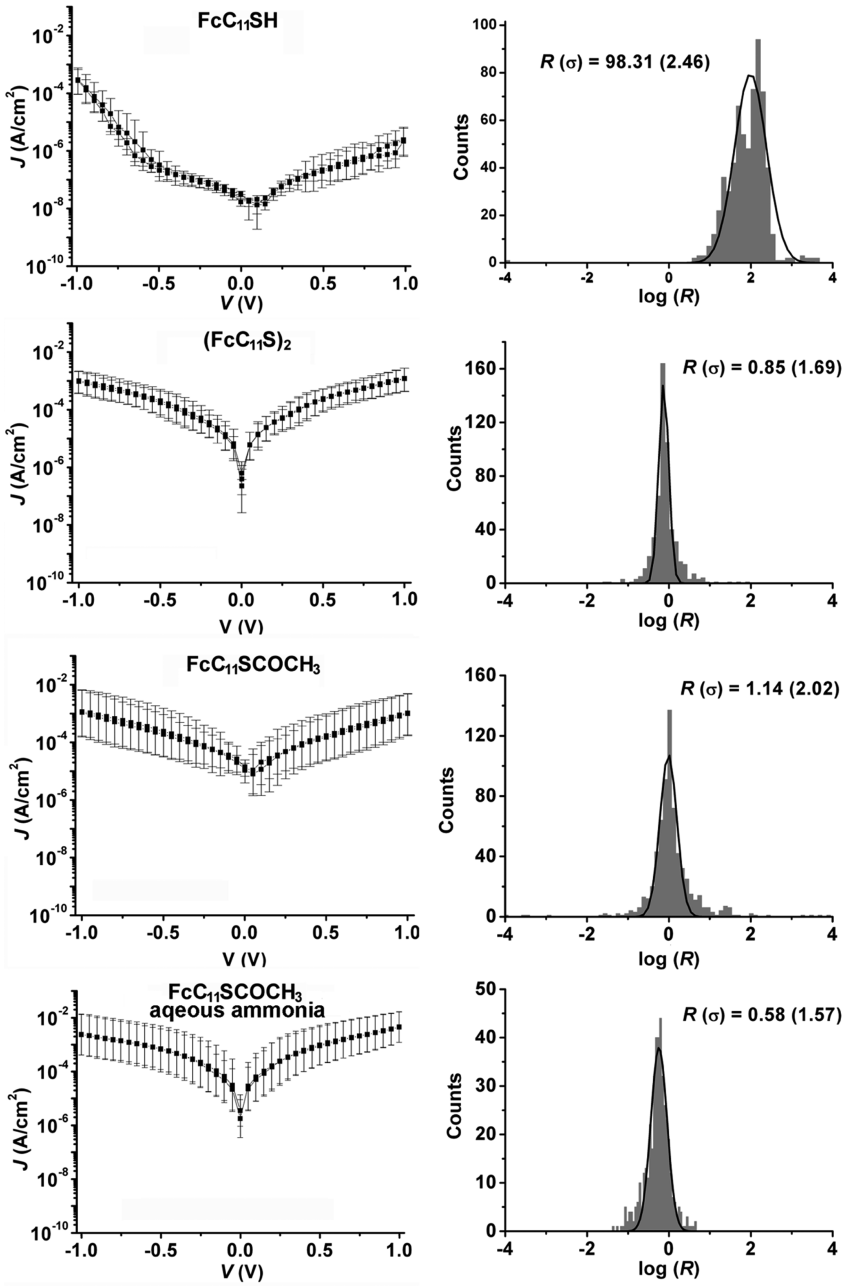

Figure 4. The average $J(V)$ curves of Ag^{TS}-$SC_{11}Fc$//GaO_x/EGaIn junctions and histograms of the values of R (= $|J(-1.0\ V)|/|J(+1.0\ V)|$) with a Gaussian fit to these histograms.

known quantities of disulfide to the thiol precursor and used this mixture to form SAMs; these SAMs were incorporated in our tunneling junctions.

We used cyclic voltammetry to determine the value of Γ_{Fc} of these mixed SAMs. Figure 6 shows that with increasing fraction of $(SC_{11}Fc)_2$, χ_{SS} (χ_{SS} = [disulfide]/([disulfide] + [thiol]), the value of Γ_{Fc} decreases (see Figure S3, Supporting Information, for the cyclic voltammograms). This result is in agreement with the results described above that $(SC_{11}Fc)_2$ forms SAMs on Au^{TS} with lower values of Γ_{Fc} than those SAMs formed with $HSC_{11}Fc$. Interestingly, Γ_{Fc} decreases sharply with increasing χ_{SS} up to 0.15 after which the surface coverage decreases more gradually with increasing values of χ_{SS} up to 1. Thus, it seems that the mixed SAMs with disulfide fractions smaller than 0.15 are dominated by the standing-up phase as normally obtained with thiols, while those SAMs obtained with disulfide fractions between 0.15 and 1 are dominated by domains of flat-lying and standing-up molecules as obtained for SAMs derived from pure disulfides.

Figure 7 shows the $J(V)$ characteristics of the SAMs (see Figure S4, Supporting Information, for all $J(V)$ curves), and Figure 8 shows the values of R, yield in nonshorting devices, and the values of J measured at +1.0 and −1.0 V as a function of χ_{SS} (see Table 3 for the statistics of the devices). We made the following three observations. (i) The performance of the molecular diodes is very sensitive to the purity of the thiol precursor in terms of rectification ratios. For instance, for χ_{SS} = 0.03 the value of R decreased by 28%, and χ_{SS} > 0.15 lowered the value of R to nearly unity. (ii) The performance of the molecular diodes is very insensitive to the purity of the thiol

dx.doi.org/10.1021/ja411116n | J. Am. Chem. Soc. 2014, 136, 1982−1991

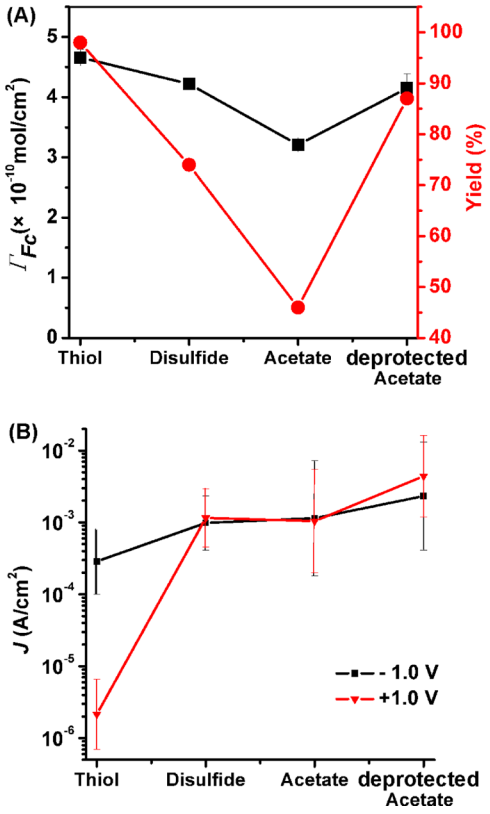

Figure 5. (A) The surface coverage determined by cyclic voltammetry of SAMs formed by different anchoring group (black) and the yield of the corresponding nonshorting devices (red). (B) The current densities measured at an applied bias of +1.0 and −1.0 V as a function of SAM precursor.

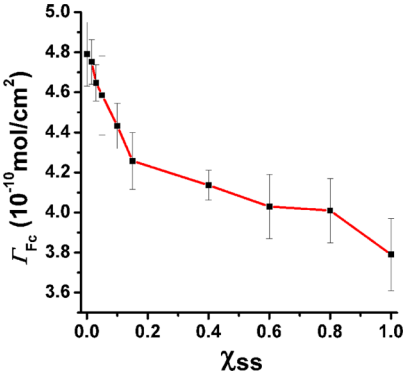

Figure 6. Surface coverage determined by cyclic voltammetry of SAMs derived from mixtures of disulfide and thiols (χ_{SS} = 0, 0.015, 0.03, 0.05, 0.10, 0.15, 0.40, 0.60, 0.80, or 1.0) on Au^{TS} electrodes determined from cyclic voltammograms measured at a scan rate of 1.0 V/s, using a Ag/AgCl reference electrode and aqueous $HClO_4$ as electrolyte.

precursor in terms of yield in nonshorting devices. The yield in nonshorting devices remains roughly constant at ∼90% for values of χ_{SS} between 0 and 0.4 despite the fact R decreases from 98 to 1. The yield in nonshorting junctions gradually decreased from 90 to 75% with increasing values of χ_{SS} between 0.6 and 1. (iii) The performance of the molecular diodes is very sensitive to the purity of the thiol precursor in terms of leakage currents. The values of J determined −1.0 V did not change as a function of χ_{SS}. In contrast, the values of J increased 2 orders of magnitude with increasing values of χ_{SS} from 0 to 0.15. The $J(V)$ data for junctions with SAM derived from thiols with χ_{SS} > 0.15 are symmetrical and not significantly different from each other. From these results we conclude that small changes in the surface coverage have a large influence on the leakage currents, which lower the rectification ratios.

CONCLUSIONS

Performance of SAM-Based Junctions Depends on the Type of the SAM-Precursor. We studied SAM-based tunnel junctions that rectify currents with ferrocene (Fc) functionalized-SAMs of the type $SC_{11}Fc$ immobilized on ultraflat silver bottom-electrodes and contacted by GaO_x/EGaIn top electrode. Junctions with thiol-based SAMs yield junctions with the best electronic performance, but those junctions with SAMs derived from disulfides, thioacetates, and in situ-deprotected thioacetates performed poorly. We found that performance relates directly to the quality of the SAMs and that only the thiols form densely packed SAMs, while the other precursors formed loosely packed SAMs that contain domains of flat-lying molecules. Many potential molecular diodes, especially those based on donor−bridge−acceptor moieties, are potentially reactive toward the free thiol functionality and therefore are restricted to use, for instance, the disulfide or thioacetate derivatives. Our results show that the interpretation of the data generated by junctions that incorporate SAMs derived from protected thiols are only reliable in combination with a careful characterization of the (supramolecular) structure of the SAMs. For similar reasons, covalent monolayers cannot self-organize as well as reversibly bound molecules and therefore have lower surface coverages. These systems are also prone to result in molecular electronic devices in which leakage currents dominate the electrical characteristics.

Performance of SAM-Based Junctions Depends on the Purity of the SAM-Precursor. One of the most common impurities of thiols is the corresponding disulfide because thiols convert to the disulfide in ambient conditions. We found that even small quantities of disulfide contamination present in the thiol derivatives have a significant effect on the device performance: 3% of disulfide impurity lowered the rectification ratio by a factor of 0.3. The junctions did not rectify when the disulfide concentration was >15%. Therefore, high purity and proper storage (inert, dark, and dry atmosphere at low temperature) of the thiols is required to ensure the formation of high quality SAMs.

Yield in Working Junctions Is a Poor Indicator of the Quality. Most studies use the yield in nonshorting junctions as an important indicator for junction quality. Our results show that the leakage currents increased by 2 orders of magnitude for poorly packed SAMs, while the yields in nonshorting junctions remained (nearly) constant. Thus, nonshorting devices are not equal to working devices or "high quality" junctions. Here we define a working junction as junction whose characteristics are dominated by the (supramolecular) structure of the SAMs and have low leakage currents. Despite a high yield in nonshorting junctions for junctions that incorporate SAMs derived from disulfides or thioacetates, these junctions cannot be classified as working junctions because they have high leakage currents. Thus to classify a junction as a "working junction", the amount of leakage currents across the junction should be known.

Leakage Currents Must Be Kept to a Minimum. Many studies used fairly complicated molecular architectures in junctions to study their electronic properties. Adding complexity may result in poorly packed SAMs and consequently in

dx.doi.org/10.1021/ja411116n | J. Am. Chem. Soc. 2014, 136, 1982−1991

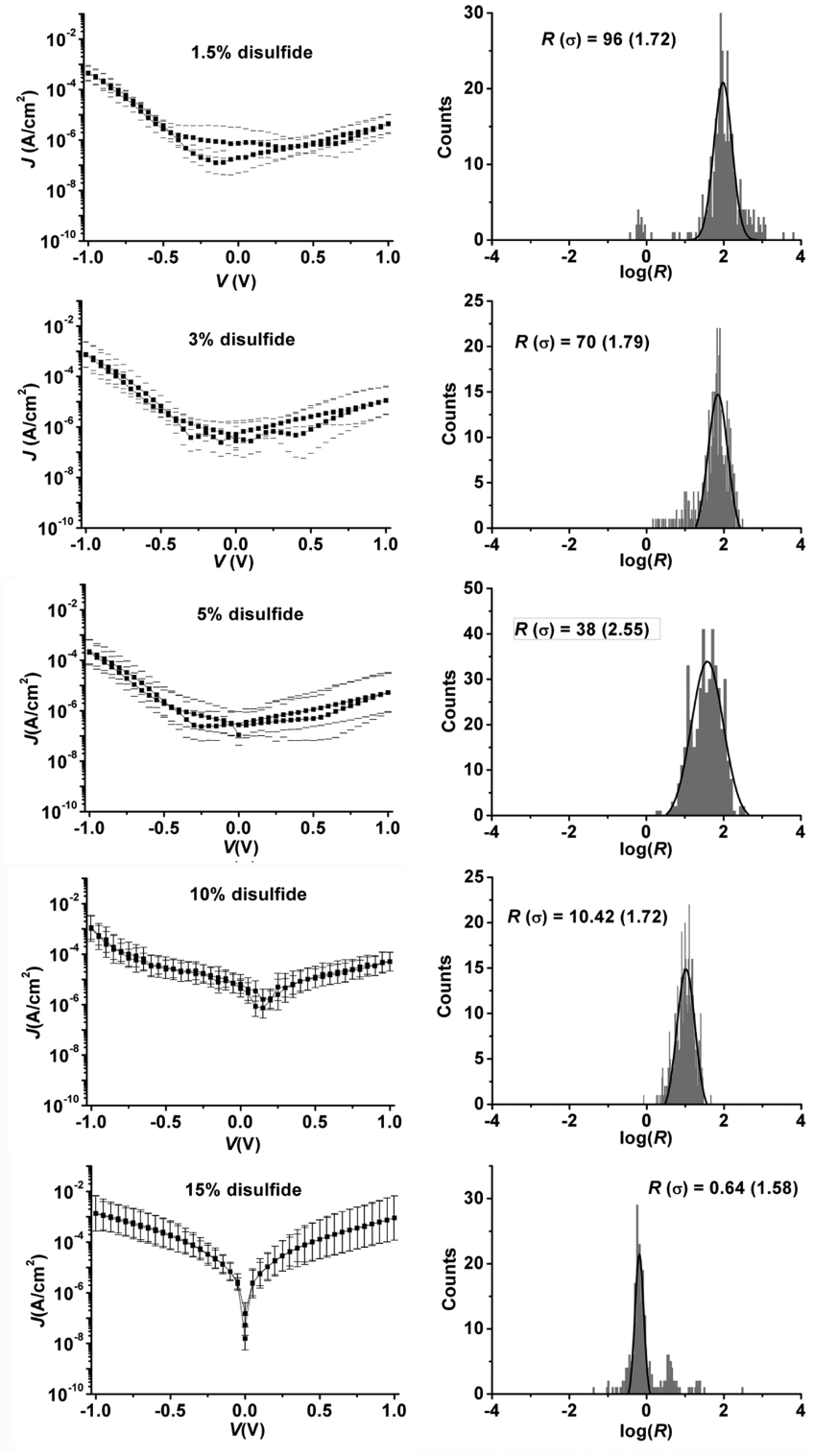

Figure 7. The average $J(V)$ curves for junctions with mixed SAMs of (χ_{SS} = 0.015, 0.03, 0.05, 0.10, and 0.15) on the left and the corresponding histograms of the values of R (= $|J(-1\ V)|/|J(+1\ V)|$) with a Gaussian fit to these histograms on the right.

devices with large leakage currents. For instance, molecular diodes of the form donor−bridge−acceptor form SAMs whose supramolecular structures are not known a priori and may result in loosely packed SAMs due to a mismatch in size of the donor−acceptor moiety and the alkyl chain. Junctions incorporating such SAMs may therefore have disappointing electrical characteristics, e.g., low rectification ratios. We have recently shown that indeed a small change in the van der Waals packing energy between the molecules in the SAMs of only 0.5 kcal/mol resulted in 10-fold change in the rectification ratio.[16] It is well-known that the packing of the molecules or polymers in thin-film devices have a dramatic effect on device performance.[15] Therefore we believe that our findings not only apply to molecular diodes, but also are generally applicable, and are important in the rational design of other

dx.doi.org/10.1021/ja411116n | J. Am. Chem. Soc. 2014, 136, 1982−1991

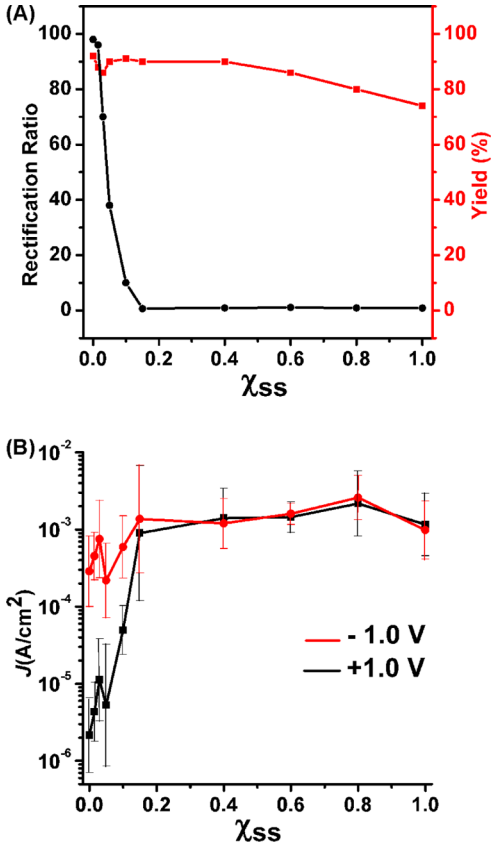

Figure 8. (A) Rectification ratio (black) and yield of nonshorting junctions (red) as a function of the fraction of $(FcC_{11}S)_2$. (B) Current density determined at a bias of +1.0 and −1.0 V as a function of fraction of disulfide (χ_{SS} = 0, 0.015, 0.03, 0.05, 0.10, 0.15, 0.40, 0.60, 0.80, or 1.0).

molecular electronic devices where it is important to minimize leakage currents.

■ ASSOCIATED CONTENT

Supporting Information

Experimental details, atomic force micrographs, angle-dependent photoelectron spectroscopy, electrical characterization of the junctions, and cyclic voltammograms. This material is available free of charge via the Internet at http://pubs.acs.org.

■ AUTHOR INFORMATION

Corresponding Author

christian.nijhuis@nus.edu.sg

Notes

The authors declare no competing financial interest.

■ ACKNOWLEDGMENTS

The Singapore National Research Foundation (NRF Award No. NRF-RF 2010-03 to C.A.N.) is kindly acknowledged for supporting this research.

■ REFERENCES

(1) Solomon, G. C.; Herrmann, C.; Ratner, M. A. *Unimolecular and Supramolecular Electronics II: Chemistry and Physics Meet at Metal-Molecule Interfaces*; Springer: New York, 2012; Vol. *313*, p 1.
(2) Akkerman, H. B.; de Boer, B. *J. Phys.: Condens. Matter* **2008**, *20*, 20.
(3) McCreery, R. L. *Chem. Mater.* **2004**, *16*, 4477.
(4) Selzer, Y.; Allara, D. L. *Annu. Rev. Phys. Chem.* **2006**, *57*, 593.
(5) Love, J. C.; Estroff, L. A.; Kriebel, J. K.; Nuzzo, R. G.; Whitesides, G. M. *Chem. Rev.* **2005**, *105*, 1103.
(6) McCreery, R. L.; Bergren, A. J. *Adv. Mater.* **2009**, *21*, 4303.
(7) Nijhuis, C. A.; Reus, W. F.; Whitesides, G. M. *J. Am. Chem. Soc.* **2009**, *131*, 17814.
(8) Ramachandra, S.; Schuermann, K. C.; Edafe, F.; Belser, P.; Nijhuis, C. A.; Reus, W. F.; Whitesides, G. M.; De Cola, L. *Inorg. Chem.* **2011**, *50*, 1581.
(9) Mentovich, E. D.; Rosenberg-Shraga, N.; Kalifa, I.; Gozin, M.; Mujica, V.; Hansen, T.; Richter, S. *J. Phys. Chem. C* **2013**, *117*, 8468.
(10) Wassel, R. A.; Credo, G. M.; Fuierer, R. R.; Feldheim, D. L.; Gorman, C. B. *J. Am. Chem. Soc.* **2004**, *126*, 295.
(11) He, J.; Lindsay, S. M. *J. Am. Chem. Soc.* **2005**, *127*, 11932.
(12) Shapir, E.; Sagiv, L.; Molotsky, T.; Kotlyar, A. B.; Di Felice, R.; Porath, D. *J. Phys. Chem. C* **2010**, *114*, 22079.
(13) Amdursky, N.; Pecht, I.; Sheves, M.; Cahen, D. *Proc. Natl. Acad. Sci. U. S. A.* **2013**, *110*, 507.
(14) Artés, J. M.; López-Martínez, M.; Giraudet, A.; Díez-Pérez, I.; Sanz, F.; Gorostiza, P. *J. Am. Chem. Soc.* **2012**, *134*, 20218.
(15) Henson, Z. B.; Müllen, K.; Bazan, G. C. *Nat. Chem.* **2012**, *4*, 699.
(16) Nerngchamnong, N.; Yuan, L.; Qi, D. C.; Li, J.; Thompson, D.; Nijhuis, C. A. *Nat. Nanotechnol.* **2013**, *8*, 113.
(17) Laibinis, P. E.; Whitesides, G. M.; Allara, D. L.; Tao, Y. T.; Parikh, A. N.; Nuzzo, R. G. *J. Am. Chem. Soc.* **1991**, *113*, 7152.
(18) Tang, X. Y.; Schneider, T.; Buttry, D. A. *Langmuir* **1994**, *10*, 2235.
(19) Tour, J. M.; Jones, L.; Pearson, D. L.; Lamba, J. J. S.; Burgin, T. P.; Whitesides, G. M.; Allara, D. L.; Parikh, A. N.; Atre, S. V. *J. Am. Chem. Soc.* **1995**, *117*, 9529.
(20) Béthencourt, M. I.; Srisombat, L. O.; Chinwangso, P.; Lee, T. R. *Langmuir* **2009**, *25*, 1265.
(21) Ulman, A. *Chem. Rev.* **1996**, *96*, 1533.
(22) McGuiness, C. L.; Blasini, D.; Masejewski, J. P.; Uppili, S.; Cabarcos, O. M.; Smilgies, D.; Allara, D. L. *ACS Nano* **2007**, *1*, 30.
(23) Onclin, S.; Ravoo, B. J.; Reinhoudt, D. N. *Angew. Chem., Int. Ed.* **2005**, *44*, 6282.
(24) Wen, K.; Maoz, R.; Cohen, H.; Sagiv, J.; Gibaud, A.; Desert, A.; Ocko, B. M. *ACS Nano* **2008**, *2*, 579.
(25) Vilan, A.; Yaffe, O.; Biller, A.; Salomon, A.; Kahn, A.; Cahen, D. *Adv. Mater.* **2010**, *22*, 140.
(26) Venkataraman, L.; Park, Y. S.; Whalley, A. C.; Nuckolls, C.; Hybertsen, M. S.; Steigerwald, M. L. *Nano Lett.* **2007**, *7*, 502.
(27) Fatemi, V.; Kamenetska, M.; Neaton, J. B.; Venkataraman, L. *Nano Lett.* **2011**, *11*, 1988.
(28) Hong, W. J.; Manrique, D. Z.; Moreno-Garcia, P.; Gulcur, M.; Mishchenko, A.; Lambert, C. J.; Bryce, M. R.; Wandlowski, T. *J. Am. Chem. Soc.* **2011**, *134*, 2292.
(29) Quek, S. Y.; Choi, H. J.; Louie, S. G.; Neaton, J. B. *ACS Nano* **2011**, *5*, 551.
(30) Long, B.; Manning, M.; Burke, M.; Szafranek, B. N.; Visimberga, G.; Thompson, D.; Greer, J. C.; Povey, I. M.; MacHale, J.; Lejosne, G.; Neumaier, D.; Quinn, A. J. *Adv. Funct. Mater.* **2012**, *22*, 717.
(31) O'Mahony, S.; Dwyer, C. O.; Nijhuis, C. A.; Greer, J. C.; Quinn, A. J.; Thompson, D. *Langmuir* **2013**, *29*, 7271.
(32) Hihath, J.; Bruot, C.; Nakamura, H.; Asai, Y.; Díez-Pérez, I.; Lee, Y.; Yu, L. P.; Tao, N. J. *ACS Nano* **2011**, *5*, 8331.
(33) Elbing, M.; Ochs, R.; Koentopp, M.; Fischer, M.; von Hanisch, C.; Weigend, F.; Evers, F.; Weber, H. B.; Mayor, M. *Proc. Natl. Acad. Sci. U. S. A.* **2005**, *102*, 8815.
(34) Ng, M. K.; Lee, D. C.; Yu, L. P. *J. Am. Chem. Soc.* **2002**, *124*, 11862.
(35) Hällback, A. S.; Poelsema, B.; Zandvliet, H. J. W. *Solid State Commun.* **2007**, *141*, 645.
(36) Metzger, R. M. *Chem. Rev.* **2003**, *103*, 3803.
(37) Honciuc, A.; Metzger, R. M.; Gong, A. J.; Spangler, C. W. *J. Am. Chem. Soc.* **2007**, *129*, 8310.
(38) Metzger, R. M. *J. Mater. Chem.* **2008**, *18*, 4364.

(39) He, H. Y.; Pandey, R.; Mallick, G.; Karna, S. P. *J. Phys. Chem. C* **2009**, *113*, 1575.
(40) Yee, S. K.; Sun, J. B.; Darancet, P.; Tilley, T. D.; Majumdar, A.; Neaton, J. B.; Segalman, R. A. *ACS Nano* **2011**, *5*, 9256.
(41) Aviram, A.; Ratner, M. A. *Chem. Phys. Lett.* **1974**, *29*, 277.
(42) Singh, R.; Whitesides, G. M. *Supplement S: The Chemistry of Sulfur-Containing Functional Groups*; Patai, S., Rappoport, Z., Eds.; J. Wiley and Sons, Ltd.: England, 1993; Vol. *13*, p 633.
(43) Suggs, J. W. *Organic Chemistry*; Barron's Educational Series, Inc.: Hauppauge, NY, 2002, p 243.
(44) Badin, M. G.; Bashir, A.; Krakert, S.; Strunskus, T.; Terfort, A.; Wöll, C. *Angew. Chem., Int. Ed.* **2007**, *46*, 3762.
(45) Park, T.; Kang, H.; Kim, Y.; Lee, S.; Noh, J. *Bull. Korean Chem. Soc.* **2011**, *32*, 39.
(46) Singh, A.; Dahanayaka, D. H.; Biswas, A.; Bumm, L. A.; Halterman, R. L. *Langmuir* **2010**, *26*, 13221.
(47) Park, T.; Kang, H.; Jeong, Y.; Lee, C.; Lee, Y.; Noh, J. *J. Nanosci. Nanotechnol.* **2011**, *11*, 4333.
(48) Azzam, W.; Bashir, A.; Shekhah, O. *Appl. Surf. Sci.* **2011**, *257*, 3739.
(49) Jeong, Y.; Chung, H.; Noh, J. *Colloids Surf., A* **2008**, *313*, 608.
(50) Riposan, A.; Liu, G. Y. *J. Phys. Chem. B* **2006**, *110*, 23926.
(51) Yang, G. H.; Liu, G. Y. *J. Phys. Chem. B* **2003**, *107*, 8746.
(52) Valkenier, H.; Huisman, E. H.; van Hal, P. A.; de Leeuw, D. M.; Chiechi, R. C.; Hummelen, J. C. *J. Am. Chem. Soc.* **2011**, *133*, 4930.
(53) Hegner, M.; Wagner, P.; Semenza, G. *Surf. Sci.* **1993**, *291*, 39.
(54) Cademartiri, L.; Thuo, M. M.; Nijhuis, C. A.; Reus, W. F.; Tricard, S.; Barber, J. R.; Sodhi, R. N. S.; Brodersen, P.; Kim, C.; Chiechi, R. C.; Whitesides, G. M. *J. Phys. Chem. C* **2012**, *116*, 10848.
(55) Thuo, M. M.; Reus, W. F.; Simeone, F. C.; Kim, C.; Schulz, M. D.; Yoon, H. J.; Whitesides, G. M. *J. Am. Chem. Soc.* **2012**, *134*, 10876.
(56) Thuo, M. M.; Reus, W. F.; Nijhuis, C. A.; Barber, J. R.; Kim, C.; Schulz, M. D.; Whitesides, G. M. *J. Am. Chem. Soc.* **2011**, *133*, 2962.
(57) Fracasso, D.; Valkenier, H.; Hummelen, J. C.; Solomon, G. C.; Chiechi, R. C. *J. Am. Chem. Soc.* **2011**, *133*, 9556.
(58) Fracasso, D.; Muglali, M. I.; Rohwerder, M.; Terfort, A.; Chiechi, R. C. *J. Phys. Chem. C* **2013**, *117*, 11367.
(59) Chiechi, R. C.; Weiss, E. A.; Dickey, M. D.; Whitesides, G. M. *Angew. Chem., Int. Ed.* **2008**, *47*, 142.
(60) Nijhuis, C. A.; Reus, W. F.; Barber, J. R.; Dickey, M. D.; Whitesides, G. M. *Nano Lett.* **2010**, *10*, 3611.
(61) Nijhuis, C. A.; Reus, W. F.; Barber, J. R.; Whitesides, G. M. *J. Phys. Chem. C* **2012**, *116*, 14139.
(62) Ricoeur, G.; Lenfant, S.; Guerin, D.; Vuillaume, D. *J. Phys. Chem. C* **2012**, *116*, 20722.
(63) Reus, W. F.; Thuo, M. M.; Shapiro, N. D.; Nijhuis, C. A.; Whitesides, G. M. *ACS Nano* **2012**, *6*, 4806.
(64) Smaali, K.; Lenfant, S.; Karpe, S.; Ocafrain, M.; Blanchard, P.; Deresmes, D.; Godey, S.; Rochefort, A.; Roncali, J.; Vuillaume, D. *ACS Nano* **2010**, *4*, 2411.
(65) Rivest, J. B.; Swisher, S. L.; Fong, L. K.; Zheng, H. M.; Alivisatos, A. P. *ACS Nano* **2011**, *5*, 3811.
(66) Masillamani, A. M.; Crivillers, N.; Orgiu, E.; Rotzler, J.; Bossert, D.; Thippeswamy, R.; Zharnikov, M.; Mayor, M.; Samori, P. *Chem.—Eur. J.* **2012**, *18*, 10335.
(67) Nijhuis, C. A.; Reus, W. F.; Whitesides, G. M. *J. Am. Chem. Soc.* **2010**, *132*, 18386.
(68) Muller-Meskamp, L.; Karthauser, S.; Zandvliet, H. J. W.; Homberger, M.; Simon, U.; Waser, R. *Small* **2009**, *5*, 496.
(69) Weiss, E. A.; Chiechi, R. C.; Kaufman, G. K.; Kriebel, J. K.; Li, Z. F.; Duati, M.; Rampi, M. A.; Whitesides, G. M. *J. Am. Chem. Soc.* **2007**, *129*, 4336.
(70) Weiss, E. A.; Kaufman, G. K.; Kriebel, J. K.; Li, Z.; Schalek, R.; Whitesides, G. M. *Langmuir* **2007**, *23*, 9686.
(71) Yu, X. J.; Wilhelmi, O.; Moser, H. O.; Vidyaraj, S. V.; Gao, X. Y.; Wee, A. T. S.; Nyunt, T.; Qian, H. J.; Zheng, H. W. *J. Electron Spectrosc. Relat. Phenom.* **2005**, *144*, 1031.
(72) Bard, A. J.; Faulkner, L. R. In *Electrochemical Methods: Fundamentals and Applications*; Wiley: New York, 1980; p 718.
(73) Rowe, G. K.; Creager, S. E. *Langmuir* **1991**, *7*, 2307.
(74) Ye, S.; Sato, Y.; Uosaki, K. *Langmuir* **1997**, *13*, 3157.
(75) Lee, L. Y. S.; Sutherland, T. C.; Rucareanu, S.; Lennox, R. B. *Langmuir* **2006**, *22*, 4438.
(76) Moulder, J. F.; Stickle, W. E.; Sobol, P. E.; Bomben, K. D. *Handbook of X-ray Photoelectron Spectroscopy*; Perkin-Elmer Corporation: Eden Prairie, MN, 1992.
(77) Cometto, F. P.; Ruano, G.; Ascolani, H.; Zampieri, G. *Langmuir* **2013**, *29*, 1400.
(78) Park, T.; Kang, H.; Choi, I.; Chung, H.; Ito, E.; Hara, M.; Noh, J. *Bull. Korean Chem. Soc.* **2009**, *30*, 441.
(79) Rodriguez, J. A.; Dvorak, J.; Jirsak, T.; Liu, G.; Hrbek, J.; Aray, Y.; González, C. *J. Am. Chem. Soc.* **2003**, *125*, 276.
(80) Cometto, F. P.; Macagno, V. A.; Paredes-Olivera, P.; Patrito, E. M.; Ascolani, H.; Zampieri, G. *J. Phys. Chem. C* **2010**, *114*, 10183.
(81) Dickey, M. D.; Chiechi, R. C.; Larsen, R. J.; Weiss, E. A.; Weitz, D. A.; Whitesides, G. M. *Adv. Funct. Mater.* **2008**, *18*, 1097.
(82) Simeone, F. C.; Yoon, H. J.; Thuo, M. M.; Barber, J. R.; Smith, B.; Whitesides, G. M. *J. Am. Chem. Soc.* **2013**, *135*, 18131.
(83) Reus, W. F.; Nijhuis, C. A.; Barber, J. R.; Thuo, M. M.; Tricard, S.; Whitesides, G. M. *J. Phys. Chem. C* **2012**, *116*, 6714.